

DYNAMICAL EVOLUTION OF THE YOUNG STARS IN THE GALACTIC CENTER:  
N-BODY SIMULATIONS OF THE S-STARSHAGAI B. PERETS<sup>1</sup>, ALESSIA GUALANDRIS<sup>2</sup>, GABOR KUPI<sup>1</sup>, DAVID MERRITT<sup>2</sup> AND TAL ALEXANDER<sup>1</sup>*Draft version February 23, 2019*

## Abstract

We use  $N$ -body simulations to study the evolution of the orbital eccentricities of stars deposited near ( $\lesssim 0.05$  pc) the Milky Way massive black hole (MBH), starting from initial conditions motivated by two competing models for their origin: formation in a disk followed by inward migration; and exchange interactions involving a binary star. The first model predicts modest eccentricities, lower than those observed in the S-star cluster, while the second model predicts higher eccentricities than observed. The  $N$ -body simulations include a dense cluster of  $10M_{\odot}$  stellar black holes (SBHs), expected to accumulate near the MBH by mass segregation. Perturbations from the SBHs tend to randomize the stellar orbits, partially erasing the dynamical signatures of their origin. The eccentricities of the initially highly eccentric stars evolve, in 20 Myr (the S-star lifespan), to a distribution that is consistent at the  $\sim 95\%$  level with the observed eccentricity distribution. In contrast, the eccentricities of the initially more circular orbits fail to evolve to the observed values in 20 Myr, arguing against the disk migration scenario. We find that 20%–30% of the S-stars are tidally disrupted by the MBH over their lifetimes, and that the S-stars are not likely to be ejected as hypervelocity stars outside the central 0.05 pc by close encounters with stellar black holes.

*Subject headings:* black hole physics — galaxies: nuclei — stars: kinematics

## 1. INTRODUCTION

In recent years, high resolution observations have revealed the existence of many young OB stars in the Galactic center (GC). Accurate measurement of the orbital parameters of these stars gives strong evidence for the existence of a massive black hole (MBH) which dominates the dynamics in the GC (Ghez et al. 1998; Eisenhauer et al. 2005; Gillessen et al. 2008). Most of the young stars are observed in the central 0.5 pc around the MBH. The young star population in the inner 0.05 pc (the “S-stars”) consists exclusively of B-stars, in an apparently isotropic distribution around the MBH, with relatively high eccentricities ( $0.3 \lesssim e \lesssim 0.95$ ; Gillessen et al. 2008). The young stars outside this region comprise O-stars in one or two disks, and present markedly different orbital properties (Levin & Beloborodov 2003; Bartko et al. 2008; Lu et al. 2009).

Since regular star formation in the region near the MBH is inhibited by tidal forces, many suggestions have been made regarding the origin of the S-stars. Many of these are probably ruled out by observations and/or by theoretical arguments (see Alexander 2005; Paumard et al. 2006, for a review). The various scenarios for the origin of the S-stars predict very different distributions for their orbits, which in principle could be constrained by observations. However, it is not clear to what extent relaxation processes can produce changes in the distribution of orbital parameters after the stars have been deposited near their current locations. Here we try to resolve this question. We use  $N$ -body simulations to follow the evolution of stellar orbits around the GC MBH for 20 Myr, starting from various initial conditions that were motivated by different models for the origin of the S-stars. However, we do not discuss here the possibility that an intermediate mass black hole was involved in the production and/or evolution

of the S-stars, which is discussed in details elsewhere (see Merritt et al. 2009, and references therein). We find our  $N$ -body results to be consistent with our analytical predictions, and compare them with current observations. We then discuss the implications for the validity of the models for the production of the S-stars. In addition we study the possible ejection of the S-stars outside the inner 0.05 pc and the contribution of such ejected stars to the population of hypervelocity stars (Brown (2008)) and to the isotropic population of B-stars observed at distances of up to 0.5 pc from the MBH (i.e. at distances similar to those of the young O/WR stellar disks, but outside of these disks at high inclinations).

In §2 we summarize the different models for the origin of the S-stars and the predictions that they make for the stellar orbits at the time when the stars are first deposited near the MBH. §3 describes the  $N$ -body simulations we carried out to follow the S-star orbital evolution starting from these initial conditions. §4 and §5 present the results of these simulations and discusses the implications for the origin of the stellar populations of B-stars in the GC and for the population of hypervelocity stars observed in the Galactic halo. §6 sums up.

## 2. MODELS FOR THE S-STARS ORIGIN

Many solutions have been suggested for the origin of the S-stars, but many of these have been effectively excluded (see Alexander 2005; Paumard et al. 2006 for a review). Here we focus on two basic models which differ substantially in their predictions for the initial orbital distribution of the S-stars and/or the time passed since their arrival/formation at their current location. These are (1) formation of the S-stars in a stellar disk close to the MBH, followed by transport through a planetary-migration-like scenario to their current positions (Levin 2007); (2) formation of the S-stars in binaries far from the MBH followed by scattering onto the MBH by massive perturbers (e.g. giant molecular clouds) and tidal disruption of the binaries (Perets et al. 2007; Perets & Alexander 2008), leaving a captured star in a tight orbit around the MBH. Binary disruption scenarios similar to (2) have been

<sup>1</sup> Weizmann Institute of Science, POB 26, Rehovot 76100, Israel<sup>2</sup> Department of Physics and Center for Computational Relativity and Gravitation, Rochester Institute of Technology, Rochester, NY 14623  
Electronic address: hagai.perets@weizmann.ac.il

proposed, in which the S-stars formed in a stellar disk (either the currently observed 6 Myr old disk, or an older, currently not observed disk) and later changed their orbits due to coherent torques through an instability of eccentric disks (Madigan et al. 2008); or through the Kozai mechanism resulting from the presence of two disks (Löckmann et al. 2008). The former of these two alternative models may not be favored since the observed disk shows only moderate eccentricities ( $\sim 0.34$ ; Bartko et al. 2008) and has too short a lifetime for these processes to be effective (Madigan et al. 2008). The latter alternative is also unlikely since the Kozai mechanism is quenched in the presence of a massive enough cusp of stars such as exists in the GC (Chang 2008; Madigan et al. 2008). Furthermore, the disk-scattering scenario could be at work only in the last  $\sim 6$  Myr if originating in the currently observed stellar disk(s), while the massive perturber scenario could be at work at the last few tens of Myr (up to the life span of the S-stars). In any case, these alternative binary-disruption scenarios imply very similar initial distributions for the captured S-stars.

In the following, we briefly discuss the initial distribution of the eccentricities and inclinations of the S-stars expected from the different scenarios for their production. The models are summarized in Table 1.

### 2.1. Binary disruption by a massive black hole

A close pass of a binary star near a massive black hole results in an exchange interaction, in which one star is ejected at high velocity, while its companion is captured by the MBH and left on a bound orbit. Such interaction occurs because of the tidal forces exerted by the MBH on the binary components. Typically, a binary (with mass,  $M_{bin}$ , and semi-major axis,  $a_{bin}$ ), is disrupted when it crosses the tidal radius of the MBH (of mass  $M_\bullet$ ), given by  $r_t = a_{bin}(M_\bullet/M_{bin})^{1/3}$ . One of the binary components is captured by the MBH (Gould & Quillen 2003) on a wide and eccentric orbit while the companion is ejected with high velocity (Hills 1988).

The capture probability and the semi-major axis distribution of the captured stars were estimated by means of numerical simulations, showing that most binaries approaching the MBH within the tidal radius  $r_t(a_{bin})$  are disrupted (Hills 1991, 1992; Gualandris et al. 2005; Bromley et al. 2006). The harmonic mean semi-major axis for 3-body exchanges with equal mass binaries was found to be (Hills 1991)

$$\langle a_{cap} \rangle \simeq 0.56 \left( \frac{M_\bullet}{M_{bin}} \right)^{2/3} a_{bin} \simeq 0.56 \left( \frac{M_\bullet}{M_{bin}} \right)^{1/3} r_t, \quad (1)$$

where  $a_{bin}$  is the semi-major axis of the infalling binary and  $a_{cap}$  that of the captured star (the MBH-star “binary”). Most values of  $a_{cap}$  fall within a factor 2 of the mean. This relation maps the semi-major axis distribution of the infalling binaries to that of the captured stars: the harder the binaries, the more tightly bound the captured stars. The periastron of the captured star is at  $r_t$ , and therefore its eccentricity is very high (Hills 1991; Miller et al. 2005),

$$e = 1 - r_t/a_{cap} \simeq 1 - 1.8(M_{bin}/M_\bullet)^{1/3} \simeq 0.94 - 0.99 \quad (2)$$

for values typical of B-type main sequence binaries and the MBH in the GC ( $M_{bin} = 6 - 30 M_\odot$ ;  $M_\bullet = 3.6 \times 10^6 M_\odot$ ;  $a_{cap} = 0.5 - 2 \times \langle a_{cap} \rangle$ ). Therefore, in order to study the evolution of S-stars from the binary disruption scenarios we assume that the initial eccentricities of S-stars are in the range  $0.94 - 0.99$  (where most are close to the mean value of 0.98).

In principle the binary disruption scenario has specific predictions for the semi-major axis distribution of the captured stars, which could also be used for constraining the model. However such distribution is highly sensitive to differences in the (unknown) binary distribution in the GC region. The prediction of high eccentricities for the captured S-stars, instead, is robust and has only a weak dependence on the mass of the binary.

The inclinations of the captured S-stars in the massive perturbers scenario (Perets et al. 2007) are likely to be distributed isotropically since the stars originate in an isotropic cusp. In the disk instability scenario (Madigan et al. 2008), however, the progenitors of the captured stars originate from a disk and therefore their inclinations should resemble that of the stellar disk, i.e. have a very limited range, of the order of the stellar disk angular thickness.

### 2.2. Planetary like migration from the young stellar disk(s)

Levin (2007) suggested that the S-stars could have formed in the currently observed stellar disk in the GC (Bartko et al. 2008; Lu et al. 2009), and then migrated inward in a way similar to planetary migration. The migration time scale expected from such a scenario could be as short as  $10^5$  yr (for type I migration), which could be comparable to (although possibly larger than; Nayakshin et al. (2007)) the lifetime of the gaseous disk. Recent analytic work (Ogilvie & Lubow (2003); Goldreich & Sari (2003); and references therein) has shown that eccentricity is likely to be damped during migration, unless eccentricity excitation occurs, which requires the opening of a clean gap in the disk. In the latter case the migration timescale might be larger (Levin 2007), possibly inconsistent with the lifetime of the gaseous disk (Nayakshin et al. 2007). It is therefore more likely that the eccentricities of the stars are damped during the migration. Even eccentricity excitation, if such took place, is unlikely to excite very high eccentricities. The mean eccentricity of the observed stars in the stellar disk is  $0.34 \pm 0.06$ . Therefore, in order to study the evolution of the S-stars following their formation in a stellar disk, we assume them to have low eccentricities, or, being conservative, moderately high eccentricities ( $e_{max} = 0.5$ ; where we use a thermal distribution of eccentricities, cut off at  $e_{max}$ ). These simulations include the less likely (Levin 2007) possibility that the stellar disk extended inward to the current region of the S-stars, in which case the S-stars were formed in-situ and did not migrate.

## 3. THE N-BODY SIMULATIONS

To test these competing models, we carried out  $N$ -body simulations of the inner Milky Way bulge using models containing a realistic number of stars. All integrations were carried out on the 32-node GRAPE cluster gravitySimulator at the Rochester Institute of Technology which adopts a parallel setup of GRAPE accelerator boards to efficiently compute gravitational forces. The direct-summation code  $\phi$ GRAPE was used (Harfst et al. 2007). The simulations used a softening radius of  $\sim 4 R_\odot$  comparable to the radius of the S-stars  $r_\star$ , so as to be able to follow even the closest encounters between stars.

Our initial conditions were based on a collisionally evolved model of a cusp of stars and stellar remnants around the GC MBH (Hopman & Alexander 2006b, hereafter HA06; see also Freitag et al. 2006). HA06 evolved the multi-mass isotropic Fokker-Planck equation representing the stellar distribution in the region extending to  $\sim 1$  pc from the MBH;

TABLE 1  
MODELS FOR THE S-STARS ORIGIN

# Origin	Initial Eccentricity	Time (Myr)	Model Probability <sup>a</sup>	Survival Fraction <sup>b</sup>	Refs. <sup>c</sup>
1 Capture following Binary disruption due to massive perturbers or to disk instability in an old non-observed disk	High ( $0.94 \leq e \leq 0.99$ )	6	0.26	0.8	1
2 Capture following Binary disruption due to disk instability in currently observed disk	High ( $0.94 \leq e \leq 0.99$ )	20	0.93	0.7	2
3 Disk formation + planetary like migration (currently observed disk)	Low ( $e \leq 0.5$ )	6	$8 \times 10^{-3}$	0.9	3
4 Disk formation + planetary like migration (possible old disk)	Low ( $e \leq 0.5$ )	20	0.06	0.8	3

<sup>a</sup>Probability for the samples of the observed and simulated S-stars to be randomly chosen from the same distribution (see text).  
<sup>b</sup>Fraction of S-stars not disrupted by the MBH during the simulation (see text).  
<sup>c</sup>(1) Madigan et al. (2008) (2) Perets et al. (2007) (3) Levin (2007)

in their models the contribution to the gravitational potential from the distributed mass is ignored. HA06 fixed the relative numbers of objects in each of four mass bins by assuming a mass function consistent with continuous star formation. The  $10M_{\odot}$  stellar-mass black holes (SBHs) were found to follow a steep,  $n(r) \sim r^{-2}$  density profile near the MBH while the lower-mass populations (main-sequence stars, white dwarfs, neutron stars) had  $n \sim r^{-\alpha}$ ,  $1.4 \lesssim \alpha \lesssim 1.5$ . The SBHs were found to dominate the mass density inside  $\sim 0.01$  pc.

Based on this model, we constructed an  $N$ -body realization containing a total of 1200 objects within 0.3 pc of the MBH: 200 “stars,” with masses of  $3M_{\odot}$ , and 1000 “black holes” with masses  $10M_{\odot}$ , around a MBH of  $3 \times 10^6 M_{\odot}$ . We set  $\alpha = 2$  for the SBHs and  $\alpha = 1.5$  for the lower-mass stars, and each density component was tapered smoothly to zero beyond 0.1 pc when computing the corresponding  $f(E)$ . Since the S-stars may have masses as high as  $\sim 10M_{\odot}$ , the higher mass stars in our simulations could also be treated as S-stars. We did not see any major differences in the evolution of the more massive and the less massive stars, and we discuss the evolution of both together.

The number of SBHs contained within a radius  $r$  in our  $N$ -body models was

$$N(< r) \approx 600 \left( \frac{r}{0.1 \text{ pc}} \right) \quad (3)$$

implying a distributed mass within 0.1 pc of  $\sim 10^4 M_{\odot}$ . This is somewhat ( $\sim 2 - 3\times$ ) lower than the mass in SBHs in the HA06 or similar (Morris 1993; Miralda-Escudé & Gould 2000; Freitag et al. 2006) models at the same radius, and a factor  $\sim 5$  lower than the *total* mass (mostly in main-sequence stars) in the Fokker-Planck models. In this sense, the rates of evolution that we infer below can be considered to be conservative.

On the other hand, we note that the late-type (old) stars that dominate the number counts in this region have a much flatter density profile than predicted by the HA06 models, possibly even exhibiting a central “hole” (Figer et al. 2003; Zhu et al. 2008). Only the B-type stars in the nuclear star cluster show a steeply-rising number density,  $\alpha = 1.1 \pm 0.3$  (Schödel et al. 2007; Gillessen et al. 2008) but they presumably constitute a negligible fraction of the total mass in this region, and in any case are far too young to have reached a collisional steady state around the MBH. While the origin of this discrepancy between models and observations is currently unresolved, it may imply that the other contributors to the distributed mass

around the MBH, including the SBHs, also have a lower density than in the Fokker-Planck models. For instance, relaxation times at the GC may be too long for collisionally relaxed steady states to have been established in the last 10 Gyr (Merriitt & Szell 2006).

Modeling of the stellar proper motion data (Trippe et al. 2008; Schoedel et al. 2009) implies a distributed mass within 1 pc of  $0.5 - 1.5 \times 10^6 M_{\odot}$ , but these data are consistent with both rising and falling mass densities within this region and the distributed mass in the inner 0.1 pc is essentially unconstrained (Schoedel et al. 2009).

Because of these uncertainties, we discuss below how our results would vary if different numbers of SBHs were assumed.

As discussed in the previous section, we studied two basic sets of initial conditions for the S-stars. In the first model we assumed that the S-stars were captured by the MBH as in the binary disruption scenario (Gould & Quillen 2003), which leaves the captured stars in highly eccentric orbits ( $> 0.94 - 0.99$ ; cf. section 2.1). Under these assumptions, the stars evolved for 6 Myr (if formed in the stellar disk) or longer (if the S-stars formed outside the central pc, i.e. not in the young stellar disk). We evolved the models for up to 20 Myr, which is comparable to the lifetime of the most massive observed S-star (S2). In the second scenario we assumed that the S-stars formed in a gaseous disk and then migrated inwards (or formed in situ in a disk extending close to the MBH). For this case we assumed the S-stars to have low eccentricities ( $< 0.5$ ), as typical of disk formation models, and to evolve for 6 Myr (the lifetime of the observed stellar disk). In order to check both scenarios we selected the stars with initially high eccentricity orbits ( $0.94 \leq e \leq 0.99$ ) and low eccentricity orbits ( $e \leq 0.5$ ) and followed their evolution for a time appropriate to their presumed origin.

In addition to these evolutionary scenarios we also studied the possibility of ejection of S-stars as hypervelocity stars, following a close encounter with a SBH in the vicinity of the MBH, as suggested by O’Leary & Loeb (2007). Our high resolution simulations can accurately follow close encounters between stars, and therefore track any resulting high velocity ejections of stars. Motivated by recent observations of B-type main sequence stars outside the inner 0.05 pc of the Galaxy, which show evidence of random orientations similar to those of the S-stars, we also looked for stars scattered to larger distances by gravitational encounters. In other words, we considered whether captured S-stars could dynamically evolve to

become the extended B-type stars population observed outside the central 0.05 pc.

Although some binaries could exist in the close regions near the MBH (Perets 2008, 2009), these are likely to be rapidly disrupted and not play an important role in the dynamical evolution of the S-stars (Perets 2009). We therefore do not include any binaries in our initial conditions for the S-stars and SBHs evolution.

#### 4. RESULTS

##### 4.1. Simulations vs. theory: resonant relaxation

We applied the correlation curve method Eilon et al. (2008) to our simulations to identify the relaxation process responsible for the dynamical evolution of the stars (Fig. 1). The method is able to detect and measure relaxation in nearly Keplerian  $N$ -body systems. In the isotropic system considered here, the angular momentum of the stars,  $J$ , evolves both due to the slow stochastic two-body relaxation (e.g. Binney & Tremaine 1987) and to the rapid resonant relaxation (RR) (Rauch & Tremaine 1996; Rauch & Ingalls 1998; Hopman & Alexander 2006a; Gürkan & Hopman 2007; Eilon et al. 2008). Two-body relaxation changes  $J$  in a random walk fashion,  $|\Delta J|/J_c = \sqrt{\tau/\tau_{NR}}$  over the long two-body relaxation time-scale  $\tau_{NR} \sim Q^2/(N \log Q)$ , where  $J_c$  is the maximal (circular orbit) angular momentum for a given energy,  $Q = M_\bullet/M_*$ ,  $N$  is the number of enclosed stars on the distance scale of interest, and time  $\tau = t/P$  is measured in terms of the orbital period on that scale. Resonant relaxation occurs when the symmetries of the potential act to constrain the stellar orbits (e.g. closed ellipses in a Kepler potential, or planar rosettes in a spherical one). As long as the symmetry is approximately maintained on the coherence timescale  $t_w$ , the stars experience coherent torques, and  $\Delta J/J_c \sim (\sqrt{N}/Q)\tau$ . In a nearly Keplerian potential, as is the case in the inner parsec of the GC, RR can change both the magnitude of  $J$  (“scalar RR”) and its direction (“vector RR”). In the Newtonian context, the coherence of scalar RR is limited by the precession of the apoapse due to the enclosed stellar mass, on a time-scale  $\tau_M \sim Q/N$ . On timescales  $\tau > \tau_M$ , the coherent change  $\Delta J(\tau_M)$  becomes the mean free path in  $J$ -space for a rapid random walk,  $|\Delta J|/J_c = \sqrt{\tau/\tau_{sRR}}$ , where  $\tau_{sRR} \sim Q \ll \tau_{NR}$ . The coherence of vector RR is self-limited by the change in the orbital orientation due to RR, and is even faster,  $|\Delta \mathbf{J}|/J_c = \sqrt{\tau/\tau_{vRR}}$ , where  $\tau_{vRR} \sim Q/\sqrt{N}$ .

Figure (1) shows the rms change in the scalar and vector angular momentum of the stars in the simulation, as a function of the time lag  $\tau$  (correlation curves), up to the maximal time lag for which the simulation can still be analyzed with high statistical confidence,  $\tau_{\max} \sim 10^4$ . In our simulation<sup>3</sup>, the scalar RR coherence time expected from theory is  $\tau_M \sim 283$  and the scalar RR timescale is  $\tau_{sRR} \sim 3.1 \times 10^5$ . The behavior of the scalar correlation curve clearly indicates that RR dominates relaxation in our GC model. The turn from the coherent phase to the random-walk phase of RR is seen at  $\tau \sim 300$ , close to the predicted value of  $\tau_M$ . The random-walk growth continues up to full randomization and saturation at  $\sim \tau_\phi$ , as expected (Eilon et al. 2008). The scalar RR timescale can be estimated directly from the simulated data

<sup>3</sup> For a spectrum of masses,  $\tau_M \sim Q/N \langle M_* \rangle$  and  $\tau_{sRR} \sim M_\bullet/M_{\text{eff}}$ , where  $\langle M_* \rangle = 8.8 M_\odot$  and  $M_{\text{eff}} = \langle M_*^2 \rangle / \langle M_* \rangle$ .  $M_{\text{eff}} \simeq 9.7 M_\odot$  for our simulation.

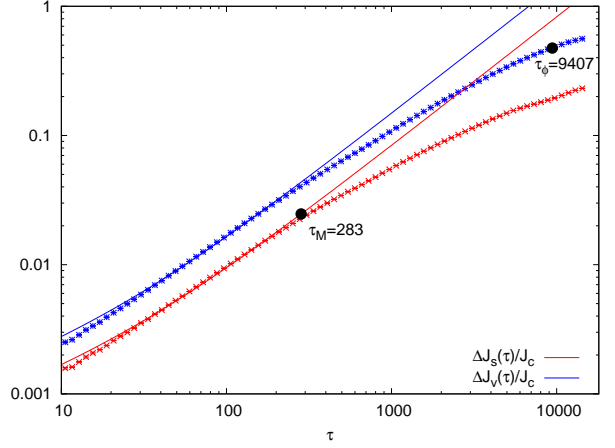


FIG. 1.— The correlation curves  $|\Delta J|/J_c$  and  $|\Delta \mathbf{J}|/J_c$  as a function of the time lag  $\tau$  for all the stars in the simulation. The simulation data (points) are compared to the best fit theoretical curves (lines). Four regimes are seen (Eilon et al. 2008, see text and also). At very short timescales, non-resonant two-body relaxation ( $\propto \sqrt{\tau}$ ) dominates over RR ( $\propto \tau$ ); At  $\tau < \tau_M$  the curves display a coherent, linear rise; At  $\tau_M < \tau < \tau_\phi$ , the curves display a random-walk growth and at  $\tau > \tau_\phi$  they begin to saturate.

by  $\tau_{RR} = \tau/(|\Delta J|/J_c)^2$ ; substituting  $|\Delta J|/J_c \sim 0.15$  at  $\tau \sim \tau_\phi/2 \sim 5000$  yields  $\tau_{sRR} \sim 2.2 \times 10^5$ , in good agreement with the predicted value.

Furthermore, since  $J/J_c = \sqrt{1 - e^2}$ , the RR-driven eccentricity evolution relates the final eccentricity,  $e_f$ , after time lag  $\tau$  to the initial eccentricity,  $e_i$ . We therefore expect the eccentricities at some given time lag to have a typical spread,  $e^-(\tau) \lesssim e_f(\tau) \lesssim e^+(\tau)$ , where

$$e^\pm(\tau) = \left[ 1 - \left( \sqrt{1 - e_i^2} \mp \sqrt{\frac{\tau}{\tau_{RR}}} \right)^2 \right]^{1/2}. \quad (4)$$

The magnitude of the predicted change in eccentricity agrees well with that observed in the simulations. For example, an S-star initially captured by a tidal exchange event on a  $P = 500$  yr ( $a \sim 0.04$  pc),  $e_i = 0.97$  orbit can evolve by RR to an  $e_f = 0.80$  orbit in 20 Myr. The short vector RR timescale  $\tau_{vRR} \sim 10^4$  ( $\tau_{vRR} = 5 \times 10^6$  yr at 0.04 pc) implies full randomization of the orbital planes after 6 Myr, throughout the S-cluster volume, as is observed in the simulation. We therefore conclude that RR is the dominant mechanism responsible for the dynamical evolution of the S-stars and other stars close to the MBH in the GC.

##### 4.2. S-star eccentricities and inclinations

In Figure 2 we show the final cumulative eccentricity distribution of the S-stars for the different origin models (Table 1). These are compared to the orbits of the observed S-stars (taken from Gillessen et al. 2008). The probabilities for the samples of the observed and simulated S-stars to be randomly chosen from the same distribution (calculated using a two-sample  $\chi^2$  test) are given in Table 1. We find that the binary disruption model taking place at least 20 Myr ago is much favored over all other models tested here. We find 93% chance for the observed S-stars and the simulated stars in such model to originate from the same distribution (with the shorter timescale of 6 Myr consistent only at the 26% level). In contrast, the disk migration scenarios seem to be excluded (for the given assumptions), since they have major difficulties in

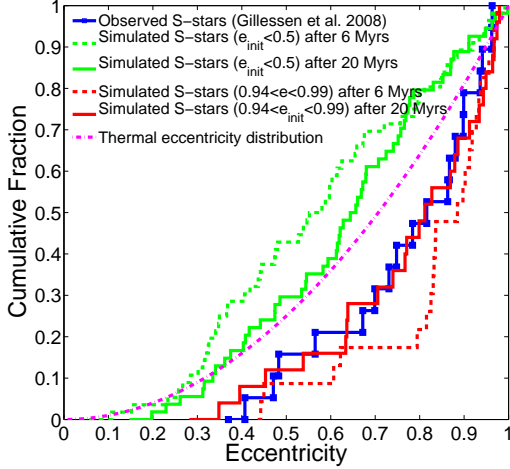


FIG. 2.— Cumulative distribution of observed and simulated S-stars eccentricities, for various models (see legend).

explaining the large fraction of eccentric orbits observed for the S-stars in the GC.

We find that the inclination distribution of the captured stars, initialized with the same inclination, is rapidly isotropized, to resemble a random distribution of inclinations (consistent with random at the  $\sim 65\%$  and  $\sim 20\%$  level, after evolution of 20 and 6 Myr, respectively). This is expected from the RR process, as discussed in the previous section (see also fig. 1). We conclude that the observed isotropic distribution of the S-stars angular momentum direction is consistent with all the S-stars production models studied here, and can not be used to discriminate between them, although it constrains the lifetime of the S-stars system to be at least  $\sim 4$  Myr at the 95% level, assuming all S-stars were initially put on the same plane.

#### 4.3. Survival of the S-stars: tidal disruption, ejection and hypervelocity stars

As already discussed above, the S-stars can change their orbits due to their dynamical evolution. A star could therefore be scattered very close to the MBH and be disrupted by it, if its pericenter distance from the MBH becomes smaller than the tidal radius of the star  $r_t = r_*(M_\bullet/m_*)^{1/3}$ . Many of the S-stars could therefore not survive for long close to the MBH. We followed the orbits of stars in our simulations and calculated the fraction of stars that have been disrupted. For the tidal disruption calculations all stars were assumed to have the typical main sequence radius according to their mass. We consider a star as being disrupted if its pericenter became smaller than twice the tidal radius during the simulation (i.e., when it is strongly affected by the MBH tidal forces or even totally disrupted in one pericenter passage). We find that most of the S-stars survived to current times in all the models (see survival fractions in 1). The S-stars population in the GC therefore gives a good representation of all the S-stars formed/captured in this region. The production rate of the S-stars required to explain current observations is therefore only slightly higher (1.2–1.3 times higher) than that deduced from current number of S-stars observed.

In principle the S-stars could be ejected by strong encounters to orbits with larger semi-major axes,

putting them outside the 0.05 pc region near the MBH (Miralda-Escudé & Gould 2000), or even ejecting them as unbound hypervelocity stars (O’Leary & Loeb 2007). The softening radius used in our simulation was  $r_{soft} = 4R_\odot$ , comparable to the radius of observed S-stars, allowing us to follow even very close encounters. Nevertheless, we find that only  $\sim 10\%$  of the stars were ejected outside of the central 0.05 pc, and even those had maximal semi-major axis in the end of the simulation not extending beyond 0.1 pc. We therefore conclude that such ejected S-stars can not explain recent observations of many B-type stars outside the central 0.05 pc (H Bartko, private communication). Moreover, none of the  $3 M_\odot$  stars in our simulations have been ejected as a hypervelocity star, suggesting that ejection of hypervelocity stars through encounters with SBHs is not an efficient mechanism (see also Perets 2009 for the related constraints on this mechanism). We note that since our simulations can be rescaled, we can probe much higher stellar densities and smaller softening radius (see next section). When such rescaling is used, in which all the 1200 stars are distributed between  $3 \times 10^{-4}$  pc to 0.1 pc (rescaling the radii by half), we find 5 stars ejected beyond 0.1 pc (to have final semi-major axis of 0.1, 0.16, 0.16, 0.21 and 0.37 pc), but none ejected as hypervelocity stars or even as slow unbound stars.

#### 5. DEPENDENCE OF THE RESULTS ON THE ASSUMED DENSITY OF SBHS

As discussed above, the density of the SBHs that are responsible for the evolution in our  $N$ -body models is not well determined. Scaling the  $N$ -body results to different assumed values of  $N$  is complicated by the fact that scalar resonant relaxation has two regimes, coherent and random walk. In our models, the transition occurs at

$$t_M \simeq QP/N \sim 3 \times 10^4 \left( \frac{N_{\text{SBH}}}{10^3} \right)^{-1} \left( \frac{P}{100 \text{ yr}} \right) \text{ yr}, \quad (5)$$

where the  $N_{\text{SBH}}^{-1}$  scaling is for scattering by SBHs of a given mass.

In the coherent regime,  $\Delta t \lesssim t_M$ , orbital angular momenta grow as

$$\frac{\Delta J}{J_c} \sim 10^{-4} \left( \frac{N_{\text{SBH}}}{10^3} \right)^{1/2} \frac{\Delta t}{P}. \quad (6)$$

In the diffusive regime,  $\Delta t \gtrsim t_M$ ,

$$\left| \frac{\Delta J}{J_c} \right| \sim \sqrt{\frac{\tau}{\tau_{\text{RR}}}} \approx 2 \times 10^{-3} \sqrt{\frac{\Delta t}{P}}, \quad (7)$$

independent of  $N_{\text{SBH}}$ .

We are interested in the orbital evolution of the S-stars over timescales of  $\Delta t \sim O(10^7)$  yr. In our simulations and those with larger  $N$ ,  $\Delta t \gg t_M$ . In this large- $N$  regime, changes in eccentricity are dominated by the diffusive relation and are therefore expected to be nearly independent of  $N$  for time scales of interest, at least up to  $N$ -values of  $\sim 10^5$  where the distributed mass begins to approach the mass of the MBH and resonant relaxation is no longer effective. Only for  $N_{\text{SBH}} \lesssim 10$  does  $t_M$  approach  $10^7$  yr and our results start depending significantly on  $N_{\text{SBH}}$ . However, such a small number of SBHs in the volume of interest is highly unlikely, and therefore our results are robust to the details of the SBH cusp model.

The  $N$ -body simulations can also trivially be rescaled by

$$r \rightarrow Ar, \quad t \rightarrow A^{3/2}t \quad (8)$$

at fixed mass. This corresponds to placing the same number of SBHs into a smaller (larger) region and integrating for a shorter (longer) time. For instance, if we rescale our simulations to three times smaller distances (in which case the stars are distributed between  $3 \times 10^{-4}$  and 0.05 pc), the integration time becomes  $\sim 5$  Myr.

## 6. SUMMARY

The approximately thermal eccentricity distribution of the S-stars near the massive black hole (MBH) in the galactic center (GC),  $N(< e) \propto e^2$ , is not naturally predicted by either of the two leading models for their production: migration of stars formed in a gaseous disk; or capture of stars following binary disruption by the MBH. The former model predicts eccentricities that are too low, the latter too high. In this paper, we followed the dynamical evolution of orbits of various eccentricities near the GC MBH, including for the first time the cluster of stellar-mass black holes (SBHs) that is expected to form around the MBH via mass segregation. We found that perturbations from the SBHs can reduce the eccentricities of initially very eccentric orbits ( $0.94 \leq e_{\text{init}} \leq 0.99$ ) into a distribution that is consistent with the observed one, in a time of approximately 20 Myr, comparable to S-star lifespans; some of the stars change their eccentricities by more than 0.5 to values as low as  $e_{\text{final}} = 0.2 - 0.4$ . We confirmed these  $N$ -body

results via a theoretical analysis of the relaxation process, and used that analysis to argue that our results are not strongly dependent on the (unknown) normalization of the SBH density near the MBH. The same mechanism is unable to convert initially low-eccentricity orbits into very eccentric ones on the same time scale, arguing against the validity of the disk migration model for the origin of the S-stars. We also found that most S-stars are not disrupted by the MBH during their lifetime, and very few are ejected outside the central 0.05 pc near the MBH, and none having a semi-major axis beyond 0.1 pc. We did not find any hypervelocity star ejected in our simulation.

Evolution toward a thermal eccentricity distribution is a natural consequence of random gravitational encounters with a population of massive perturbers. In this paper, we considered the effect of a background of SBHs, which are expected on the basis of very general arguments to contribute a total mass of  $\sim 10^4 M_\odot$  in the inner 0.1 pc around the MBH. We showed that they were effective at moderating the eccentricities of initially highly eccentric orbits. These results strengthen models in which the S-stars form from disrupted binaries, and disfavor models in which the S-stars are formed with low eccentricities.

This work was supported by grants NASA NNX07AH15G, NSF AST-0821141, and NSF AST-0807810 to D. M., and by ISF grant 928/06 and Starting Grant 202996 to T. A.

## REFERENCES

- Alexander, T. 2005, *Phys. Rep.*, 419, 65  
 Bartko, H. et al. 2008, *ApJ*, in press (arXiv:0811.3903)  
 Binney, J. & Tremaine, S. 1987, *Galactic Dynamics* (Princeton, NJ: Princeton University Press)  
 Bromley, B. C. et al. 2006, *ApJ*, 653, 1194  
 Brown, W. R. 2008, arXiv:0811.0571  
 Chang, P. 2008, arXiv:0811.0829  
 Eilon, E., Kupi, G., & Alexander, T. 2008, arXiv:0807.1430  
 Eisenhauer, F. et al. 2005, *ApJ*, 628, 246  
 Figer, D. F. et al. 2003, *ApJ*, 599, 1139  
 Freitag, M., Amaro-Seoane, P., & Kalogera, V. 2006, *ApJ*, 649, 91  
 Ghez, A. M. et al. 1998, *ApJ*, 509, 678  
 Gillessen, S. et al. 2008, arXiv:0810.4674  
 Goldreich, P. & Sari, R. 2003, *ApJ*, 585, 1024  
 Gould, A. & Quillen, A. C. 2003, *ApJ*, 592, 935  
 Gualandris, A., Portegies Zwart, S., & Sipior, M. S. 2005, *MNRAS*, 363, 223  
 Gürkan, M. A. & Hopman, C. 2007, *MNRAS*, 379, 1083  
 Harfst, S. et al. 2007, *New Astronomy*, 12, 357  
 Hills, J. G. 1988, *Nature*, 331, 687  
 —. 1991, *AJ*, 102, 704  
 —. 1992, *AJ*, 103, 1955  
 Hopman, C. & Alexander, T. 2006a, *ApJ*, 645, 1152  
 —. 2006b, *ApJ*, 645, L133  
 Levin, Y. 2007, *MNRAS*, 374, 515  
 Levin, Y. & Beloborodov, A. M. 2003, *ApJ*, 590, L33  
 Löckmann, U., Baumgardt, H., & Kroupa, P. 2008, *ApJ*, 683, L151  
 Lu, J. R. et al. 2009, *ApJ*, 690, 1463  
 Madigan, A.-M., Levin, Y., & Hopman, C. 2008, arXiv:0812.3395  
 Merritt, D., Gualandris, A., & Mikkola, S. 2009, *ApJ*, 693, L35  
 Merritt, D. & Szell, A. 2006, *ApJ*, 648, 890  
 Miller, M. C. et al. 2005, *ApJ*, 631, L117  
 Miralda-Escudé, J. & Gould, A. 2000, *ApJ*, 545, 847  
 Morris, M. 1993, *ApJ*, 408, 496  
 Nayakshin, S., Cuadra, J., & Springel, V. 2007, *MNRAS*, 379, 21  
 Ogilvie, G. I. & Lubow, S. H. 2003, *ApJ*, 587, 398  
 O’Leary, R. M. & Loeb, A. 2007, *MNRAS*, 1076  
 Paumard, T. et al. 2006, *ApJ*, 643, 1011  
 Perets, H. B. 2008, arXiv:0802.1004  
 —. 2009, *ApJ*, 690, 795  
 Perets, H. B., & Alexander, T. 2008, *ApJ*, 677, 146  
 Perets, H. B., Hopman, C., & Alexander, T. 2007, *ApJ*, 656, 709  
 Rauch, K. P. & Ingalls, B. 1998, *MNRAS*, 299, 1231  
 Rauch, K. P. & Tremaine, S. 1996, *New Astronomy*, 1, 149  
 Schödel, R. et al. 2007, *A&A*, 469, 125  
 Schoedel, R., Merritt, D., & Eckart, A. 2009, arXiv:0902.3892  
 Trippe, S. et al. 2008, *A&A*, 492, 419  
 Zhu, Q. et al. 2008, *ApJ*, 681, 1254